INSTITUTE OF PHYSICS PUBLISHING JOURNAL OF PHYSICS: CONDENSED MATTER

J. Phys.: Condens. Matter **15** (2003) 1951–1961 PII: S0953-8984(03)58454-5

The effect of Mn substitution on the structure and magnetic properties of $Se(Cu_{1-x}Mn_x)O_3$ solid solution

R Escamilla[1], A Durán[1], M I Rosales[1], E Morán[2] and M A Alario-Franco[2]

[1] Instituto de Investigaciones en Materiales, Universidad Nacional Autónoma de México, 04510 México DF, Mexico
[2] Laboratorio Complutense de Altas Presiones and Departamento de Química Inorgánica, Facultad de Ciencias Químicas, Universidad Complutense, 28040-Madrid, Spain

E-mail: rauleg@servidor.unam.mx (R Escamilla Guerrero)

Received 17 January 2003
Published 17 March 2003
Online at stacks.iop.org/JPhysCM/15/1951

Abstract

The effects of Mn substitution on the structure and magnetic properties of the $SeMO_3$ ($M = Cu_{1-x}Mn_x$) solid solution have been studied. Rietveld refinements of the x-ray diffraction patterns of these samples indicate that the manganese ions occupy copper sites. This replacement induces significant changes in the M–O bond lengths that give rise to abrupt decreases of the [M–O_6] octahedral distortion. In contrast, the M–O(1)–M and M–O(2)–M bond angles remain essentially constant. The magnetic behaviour of this solid solution was studied in the temperature range of 2 K $< T <$ 300 K. The temperature dependence of the inverse magnetic susceptibility is well described by the Curie–Weiss law at high temperatures, in the composition range studied. We found that the substitution of Mn for Cu induces a sharp drop in the saturation moment of $SeCuO_3$. At about 10% of Mn there is a change from positive to negative Weiss constant θ_W that is mainly due to the [M–O_6] octahedral distortion introduced by the substitution of the larger Mn ions in the structure. The M–H isotherms show a weak ferromagnetism at about 52 K in $SeMnO_3$.

1. Introduction

Perovskite transition-metal oxides (TMO) have a long history of research and have long been known as materials with a variety of interesting properties, such as their dielectric, magnetic, optical, and transport properties. Renewal of interest in the perovskite TMO arose after the discovery of high-T_c superconductors [1], and the mechanism of superconductivity and the basic properties of the strongly correlated systems have been discussed intensively. In addition to the high-T_c-related activities, there have been very important activities in perovskite manganites. Colossal magnetoresistance [2–6], magnetic field-induced structural

phase transitions [7], and highly unique phase diagrams in the T–H plane [8] are examples of dramatic discoveries. It is true that many of the basic ingredients in the mechanisms responsible for these phenomena have been proposed in the past, such as double exchange [9–11], the Jahn–Teller effect (JT) [12–14], charge ordering [15, 16], and orbital ordering [17–19]. Nevertheless, a coherent understanding of various phenomena requires detailed analysis of the real controlling mechanism for each phenomenon, because different mechanisms can lead to the same phenomena.

Recently, study of the crystal chemistry of low-dimensional compounds has been intensive worldwide, owing to their specific and sometimes exotic magnetic properties. One way of obtaining low-dimensional compounds is to use the so-called 'lone-pair' cations, i.e., As^{III+}, Se^{IV+}, Sn^{II+}, Sb^{III+}, Te^{IV+}, Pb^{II+}, Bi^{III+} [20–22]. The copper (II)–selenium (IV)–oxygen system has been investigated and a few phases characterized: $CuSe_2O_5$ [23], $CuSeO_3$, $Cu_2O(SeO_3)$, and $Cu_4O(SeO_3)_3$ [24, 25]. In the same way, selenites or diselenites of manganese in various oxidation states (II, III, IV) have been previously described [26–30]. In all cases, the compounds have been synthesized at atmospheric pressure.

The $SeCuO_3$ and $SeMnO_3$ perovskites have been synthesized at high pressure [31]. The $SeMO_3$ ($M = Cu_{1-x}Mn_x$) perovskite adopts a distorted (ABO_3) structure, in which the Se^{IV+} cations occupy the larger A cation sites and the M^{II+} are in the B sites. In these selenites, the structural chemistry is very dependent upon the 'lone pair' on the selenium (IV); e.g., the Se^{IV+} ions with a relatively small size and strong covalent character attract three of the twelve surrounding oxygens, while the others are far apart and linked to other Se and M ions. On the other hand, the electronic 'lone pairs' of Se atoms are stereochemically active, pointing towards the empty spaces of the various networks: cavities, tunnels, or inter-sheet spaces [32–34]. Thus, a $[SeO_3]^{II-}$ group rather than a Se^{IV+} ion surrounded by twelve oxygens is the usual component of the structure of $SeMO_3$. Due to this characteristic in the coordination of Se^{IV+}, the structure of $SeMO_3$ shows Se–O–Se bond angles (120°–130°) much smaller than those observed in any of the ABO_3 perovskites (150°–180°). In addition to the above tilting, in the $SeCuO_3$ perovskite, the [Cu–O_6] octahedra also shows a large distortion with Cu–O bond lengths varying (1.9–2.6 Å) due to the JT effect in Cu^{II+} (d^9) [31].

On the other hand, the mixed-valence manganites ($RE_{1-x}A_x$)MnO_3 (RE = rare-earth cation, A = alkali or alkaline-earth cation), also having a perovskite structure, exhibit a rich variety of crystallographic, electronic, and magnetic properties. Changes in the magnetic properties seem to be associated with structural changes that have been the subject of a wide range of studies [35–37]. In the $Sr_xCa_{1-x}RuO_3$ perovskites, the variation of the magnetic properties may be basically understood as a function of the average ⟨Ru–O–Ru⟩ bond angle, but there may be other influences as well. Consideration of the A-site atom size disorder may be important; for example it has been shown that at the same doping level and mean A-site cation radius, the T_c of superconducting copper oxides and the Curie transition temperature of manganate ferromagnets both show a strong linear decrease with A-site disorder [38–40].

Both in experimental and theoretical studies (the Kramers–Anderson model [41] and Anderson–Goodenough–Kanemori (AGK) rules [42]) of the TMO with unpaired electrons in e_g orbitals, it has been reported that the magnetic interactions change from antiferromagnetic (AFM) to ferromagnetic (FM) as the ⟨B–O–B⟩ bond angle varies from 180° to 90°. Recently, Subramanian *et al* [43] have shown that in the $Se_{1-x}Te_xCuO_3$ system there is a transition from FM (for $x = 0.0$) to AFM ($x = 1.0$) that appears to be controlled by a single microscopic parameter, the ⟨Cu–O(2)–Cu⟩ bond angle, allowing for the first time a precise determination of the angle of crossover ($\alpha_c = 127° \pm 0.5°$) between the FM and AFM superexchange.

In this paper we report the effect of Mn substitution on the structure and magnetic properties of the $Se(Cu_{1-x}Mn_x)O_3$ solid solution. We also then establish a correlation between

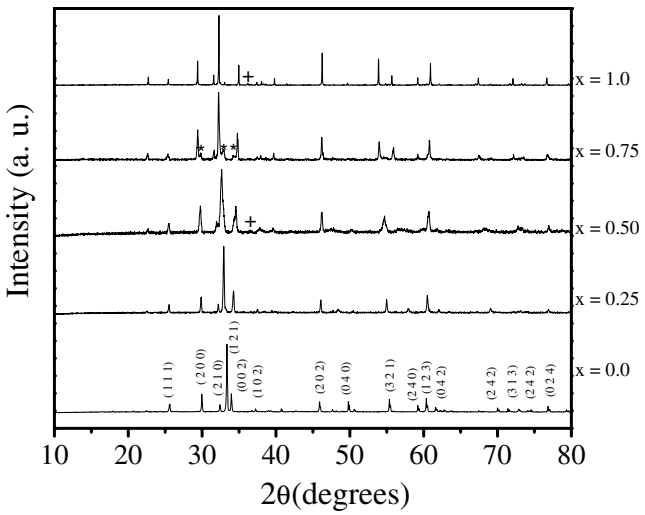

Figure 1. X-ray diffraction patterns of the $Se(Cu_{1-x}Mn_x)O_3$ ($0 \leqslant x \leqslant 1.0$) samples. The symbols represent (∗) Mn_2O_3 and (+) Mn_3O_4.

the structural parameters and magnetic changes when the Mn content is increased in the $Se(Cu_{1-x}Mn_x)O_3$ structure. We found from magnetization data that at very low Mn content a change of sign in the paramagnetic interaction parameter (θ_W) derived from the Curie–Weiss law takes place. The change of sign in this parameter can be basically understood in terms of the variation of octahedral distortion, contrary to previous assumptions that θ_W is mainly influenced by the M–O–M bond angle. From $M(H)$ curves we found a weak-ferromagnet (WFM) transition at about 52 K in the $SeMnO_3$ compound.

2. Experimental details

Different members of the $Se(Cu_{1-x}Mn_x)O_3$ system ($0 \leqslant x \leqslant 1$) have been synthesized from SeO_2, MnO, and CuO precursor oxides (99.999% purity) mixed in stoichiometric amounts, sealed in a gold capsule and heated under a pressure of 6 GPa at a temperature of 900–1000 °C using a belt-type press. Phase identification of the samples was done with an x-ray diffractometer, Siemens D5000, using Cu Kα radiation and a Ni filter. Intensities were measured in steps of 0.02° for 14 s in the 2θ range 10°–120° at room temperature. Crystallographic parameters were refined using a Rietveld refinement program, Rietica v 1.7.7 [44], with multi-phase capability. The bond valence sum was used to distinguish the oxidation states of the metals [45]. Measurements of the DC magnetization as a function of temperature and external magnetic field, $M(T, H)$, were performed in a Quantum Design SQUID at temperatures from 2 to 300 K and in an external magnetic field up to 2 T.

3. Results and discussion

Figure 1 shows the powder x-ray diffraction patterns obtained for the $Se(Cu_{1-x}Mn_x)O_3$ samples. The main features of the powder x-ray diffraction patterns of our samples correspond to the common distorted perovskite-type $SeCuO_3$ (IDDE No 31-0479) and $SeMnO_3$ (IDDE No 31-0830) structures. For $x = 0.75$, faint features of Mn_2O_3 (IDDE No 41-1442) appear,

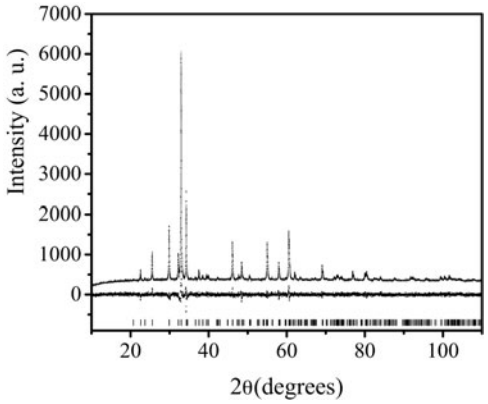

Figure 2. Rietveld refinement of the x-ray diffraction pattern for the $x = 0.25$ sample. The experimental diagram (dots), the calculated pattern (continuous curve), their difference (middle curve), and calculated peak positions (bottom).

whereas for $x = 0.5$ and 1.0, additional peaks corresponding to Mn_3O_4 (IDDE No 24-0734) can also be observed. The x-ray diffraction patterns were Rietveld fitted using an orthorhombic $\sim\sqrt{2}a_p \times 2a_p \times \sqrt{2}a_p$ $GdFeO_3$-type model within space group *Pnma* (No 62) (a_p is the cubic perovskite cell parameter). In the process of refinement, the substitution of Mn ions in the Cu sites and the quantification of the Mn_2O_3 and Mn_3O_4 phases were considered. As an example, one of the fitted patterns ($x = 0.25$) is shown in figure 2. Detailed results of the structural refinements are listed in table 1. Figure 3 shows the evolution, at room temperature, of the lattice parameters and unit-cell volume for the $Se(Cu_{1-x}Mn_x)O_3$ samples as a function of Mn content (x). We can observe that, as x is increased, the c-axis lattice parameter decreases slightly and the b-axis one increases continuously, while that the a-axis lattice parameter remains essentially constant; as a consequence of these changes, the unit-cell volume increases as a function of the Mn content. The lattice parameters obtained in this work for samples of the $SeCu_{1-x}Mn_xO_3$ system agree satisfactorily with the data available in the literature for the end-members [31]. To explain the increase in the cell volume, the ionic radii of the ions Cu^{II+} and Mn^{II+} with the coordination number 6 are taken into account; in the case of Cu^{II+} the ionic radius is 0.87 Å, while those of the Mn^{II+} in the low-spin state and high-spin state are 0.81 and 1.0 Å respectively [46]. From these values, the linear increase of the unit-cell volume is explained by the increase in the content of Mn ions in the high-spin state (see table 1).

Table 2 shows the M–O bond lengths obtained from the refined atomic positions together with the [M–O_6] octahedral distortion for each sample (see figure 4). Our results from the Rietveld fit for the $SeCu_{1-x}Mn_xO_3$ system show that the M–O average bond length changes from 2.176 ($x = 0.0$) to 2.236 Å ($x = 1.0$). In the literature, we observe that the average Mn–O bond lengths expected for [Mn^{II+}–O_6] and [Mn^{III+}–O_6] octahedra are 2.205 Å [47] and 2.023 Å [48]. In the $SeCu_{1-x}Mn_xO_3$ system, the average M–O bond lengths are 2.192 ($x = 0.25$), 2.207 ($x = 0.50$), 2.229 ($x = 0.75$), and 2.236 Å ($x = 1.0$), clearly revealing a divalent state for Mn. Moreover, the bond valence sums for these Mn contents are 2.32, 2.10, 1.90, and 1.82 vu (valence units) respectively (see table 1). It is well known that tilting is commonly observed in perovskites, such as in orthorhombic $GdFeO_3$ [49]. In the $(RE_{1-x}A_x)MnO_3$ (RE = rare-earth cation, A = alkali or alkaline-earth cation) system, the presence of the tilting is manifested by an increase of the ⟨Mn–O–Mn⟩ bond angle due

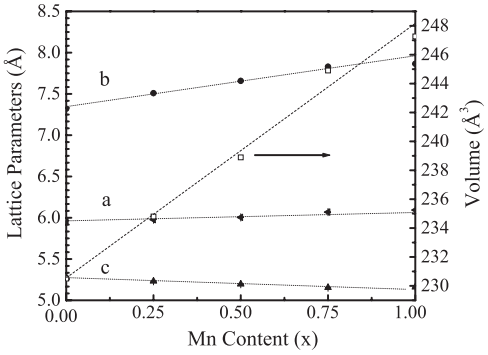

Figure 3. The crystal lattice parameters (left) and unit-cell volume (right) as a function of the Mn content (x).

Table 1. Structural parameters for $SeMO_3$ at 295 K. M = $(Cu_{1-x}Mn_x)$. Notes: space group: *Pnma* (No 62); atomic positions: M: 4b (0, 0, $\frac{1}{2}$); Se: 4c (x, $\frac{1}{4}$, z); O(1): 4c (x, $\frac{1}{4}$, z); O(2): 8d (x, y, z); S_{ij} is the bond valence sum [45].

	(x)	0.0	0.25	0.5	0.75	1.0
	a (Å)	5.9643(3)	5.9772(2)	6.0044(4)	6.0690(3)	6.0937(5)
	b (Å)	7.3204(4)	7.5095(3)	7.6581(6)	7.8299(4)	7.8651(4)
	c (Å)	5.2794(2)	5.2311(2)	5.1954(3)	5.1538(2)	5.1434(5)
	$b/\sqrt{2}$	5.1763	5.3100	5.4151	5.5366	5.5615
	V (Å^3)	230.504 21	234.80(3)	238.90(6)	244.91(5)	247.27(5)
Cu/Mn	B (Å^2)	0.20(4)	0.11(4)	1.03(5)	0.68(2)	0.3(4)
Mn	S_{ij} (vu)	—	2.32	2.1	1.90	1.82
Se	x	0.0407(6)	0.0370(4)	0.0332(3)	0.0295(2)	0.0257(3)
	z	0.0029(4)	—	—	—	—
	B (Å^2)	0.39(2)	0.0022(2)	0.0072(3)	0.0122(3)	0.0172(4)
			2.09(3)	1.17(4)	0.55(2)	0.41(4)
O(1)	x	0.0791	0.0793	0.0795	0.0797(3)	0.0798(5)
	z	0.3315(3)	0.3240(4)	0.3178(3)	0.3110(4)	0.3089(6)
	B (Å^2)	0.23(3)	1.24(3)	0.16(4)	0.17(3)	0.30(4)
O(2)	x	0.2023(2),	0.1966(2),	0.1909(2),	0.1852(4)	0.1794(4)
	y	0.0728(2),	0.0755(3),	0.0782(4),	0.0809(5)	0.0836(3)
	z	0.9066(1)	0.8982(4)	0.8890(4)	0.8790(3)	0.8692(4)
	B (Å^2)	0.23(3)	1.24(3)	0.16(4)	0.17(3)	0.30(4)
Mn_2O_3[a]		—	—	—	8%	—
Mn_3O_4[a]		—	—	4%	—	3%
	R_p (%)	6.6	4.9	6.2	9.9	16.3
	R_{wp} (%)	9.6	6.3	8.1	12.9	20.3
	R_{exp} (%)	4.9	4.9	5.7	8.3	11.8
	χ^2 (%)	3.7	1.6	2.0	2.4	2.9

[a] Percentage of impurity in the phase.

to an A-site atom size effect [35–37, 50], while in the $Sr_x(Na_{0.5}Ln_{0.5})RuO_3$ system, the ⟨Ru–O–Ru⟩ bond angle slightly increases as a direct consequence of the charge disorder on the A site [51]. Our results from the Rietveld fit for the $SeCu_{1-x}Mn_xO_3$ system show that the average ⟨M–O–M⟩ (M = $Cu_{1-x}Mn_x$) bond angles remain essentially constant: 125.5° (x = 0.0) to 125.2° (x = 1.0) (see table 2). On the other hand, Kohn *et al* [31] have shown that a large octahedral distortion observed in the $SeCuO_3$ system is due to the preference of a JT

Table 2. M–O (Å) and Se–O (Å) bond lengths, octahedral distortion (Δ_{oct}), and the [M–O_6] (M = $Cu_{1-x}Mn_x$) angles (deg) for $SeMO_3$. Note: the octahedral distortion is defined as $\Delta_{oct} = 10 \times (\sum |(\text{M–O}_i) - \langle \text{M–O} \rangle_{\text{average}}|)/\langle \text{M–O} \rangle_{\text{average}}$ [20].

x	0.0	0.25	0.5	0.75	1.0
M–O(1): 2	2.089(1)	2.144(4)	2.189(1)	2.239(3)	2.251(3)
M–O(2): 2	2.520(4)	2.458(1)	2.399(3)	2.341(4)	2.288(4)
M–O(2): 2	1.918(4)	1.973(1)	2.034(3)	2.107(4)	2.168(4)
$\langle \text{M–O} \rangle_{\text{average}}$	2.176	2.192	2.207	2.229	2.236
Δ_{oct}	3.16	2.43	1.74	1.09	0.60
M–O(2)–M: 4	127.1(1)	127.0(2)	127.0(1)	126.9(2)	126.9(3)
M–O(1)–M: 2	122.4(1)	122.2(2)	122.1(1)	121.9(3)	121.7(4)
$\langle \text{M–O–M} \rangle_{\text{average}}$	125.5	125.4	125.3	125.3	125.2
$\text{Se–O(1)}_{\text{i}}$	1.750(3)	1.735(2)	1.724(1)	1.712(1)	1.709(3)
$\text{Se–O(1)}_{\text{iv}}$	3.552(4)	3.524(2)	3.506(3)	3.483(4)	3.482(3)
$\text{Se–O(1)}_{\text{iii}}$	3.328(3)	3.370(3)	3.421(3)	3.491(3)	3.543(4)
$\text{Se–O(1)}_{\text{ii}}$	2.889(2)	2.887(1)	2.892(4)	2.914(4)	2.921(3)
$\text{Se–O(2)}_{\text{ii}}$ (×2)	1.694(4)	1.705(4)	1.712(4)	1.724(3)	1.712(1)
$\text{Se–O(2)}_{\text{vi}}$ (×2)	2.813(4)	2.869(1)	2.919(3)	2.982(1)	3.004(3)
$\text{Se–O(2)}_{\text{iii}}$ (×2)	3.230(3)	3.181(2)	3.138(4)	3.108(4)	3.073(4)
$\text{Se–O(2)}_{\text{vii}}$ (×2)	3.532(2)	3.587(3)	3.641(2)	3.706(3)	3.750(3)
Average Se–O bond length in SeO_3 group[a]	1.713	1.715	1.716	1.720	1.711

[a] With $\text{Se–O(1)}_{\text{i}}$ and $\text{Se–O(2)}_{\text{ii}}$ (×2).

Cu^{II+} ion for non-octahedral bonding. Distortions of the same type also have been observed for example in $KCuF_3$ [52] and $CuTe_2O_5$ [53]. Our results for the $SeCu_{1-x}Mn_xO_3$ system show that the octahedral distortion decreases abruptly with increasing x ($\Delta_{oct} = 3.16$ to 0.60; see figure 4). This can definitely be attributed to the number of JT Cu^{II+} ions decreasing; obviously, for $SeMnO_3$ the JT effect is zero, due to the d^5 electron configuration of the Mn^{II+} ions.

The three minimum bond lengths between selenium and oxygen ions: Se–O(1) and Se–O(2) (×2), are shown in table 2, This is a consequence of the activity of lone-pair electrons of the Se^{IV+} atoms. The average Se–O bond length calculated for this $[SeO_3]^{II-}$ group is approximately 1.71 Å. This is in accordance with the geometries found in many other selenite compounds and with average values cited in the literature [32–34, 54], which do not change for the whole range of solid solutions studied. This suggests that the substitution of Cu^{II+} ions for Mn^{II+} ions does not affect the $[SeO_3]^{II-}$ group in the $SeCu_{1-x}Mn_xO_3$ structure.

Figure 5 shows the temperature-dependent magnetization of $Se(Cu_{1-x}Mn_x)O_3$ compounds in an applied field of 1 T, for $x = 0$, 0.25, 0.50, 0.75, and 1.0, from 300 to 2 K. We can observe that the $x = 0$ end-member displays a saturation moment of 0.8 μ_B fu^{-1} which is slightly smaller than that for the isolated Cu^{II+} ion ($2S = 1$ μ_B), whereas the magnetization of $SeMnO_3$ is lower ($\sim$0.12 μ_B) than the theoretical saturated value of the isolated Mn^{II+} ion ($2S = 5$ μ_B). From $\sim$75 to 2 K, the magnetization behaviour does not show a systematic dependence on x, in contrast with the situation for doped systems previously reported in [54]. The substitution of Cu for Mn drastically decreases the saturation moment—passing from $\sim$0.8 μ_B fu^{-1} for $SeCuO_3$ to $\sim$0.11 μ_B fu^{-1} for $x = 0.25$ with a slight variation at the end composition ($\sim$0.12 μ_B fu^{-1} for $SeMnO_3$). The magnetization curves show crossing for $x = 0.25$, 0.50, and 0.75 with the smallest magnetization for $x = 0.75$ at 2 K. The inset in figure 5 shows the derivative of the magnetization, dM/dT, for all compositions. We observed for $x = 0$ and 0.25 the presence of a peak at $\sim$25.5 K. For $x = 0.50$ two peaks are present, the first at 25.5 K and the second one at about 40 K, whereas for $x = 0.75$ we observed two

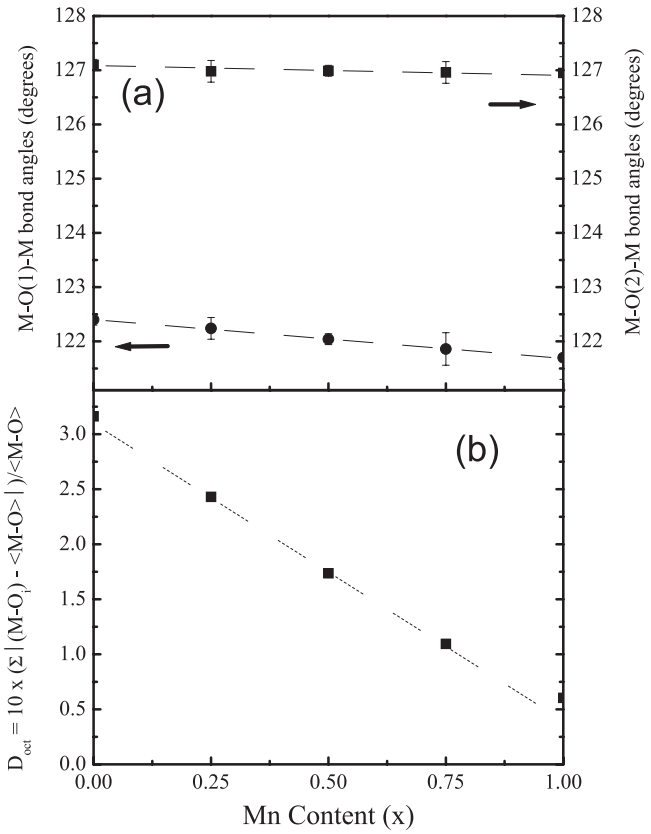

Figure 4. ⟨M–O(1)–M⟩ and ⟨M–O(2)–M⟩ bond angles versus Mn content x (a) and [M–O_6] octahedral distortion versus Mn content x (b).

peaks, at 25.5 and 52 K. For the end composition ($x = 1.0$) we observed two well-defined peaks at ∼44 and ∼52 K. The peak observed at 25.5 K is associated with FM transitions (in agreement with earlier data reported in [31]), the peaks observed at 40 and 44 K are attributed to the ferrimagnetic transition of the Mn_3O_4 phase [55] (see table 1), and below 52 K an AFM transition has been observed in $SeMnO_3$ [31].

Figure 6 shows the magnetization curves, $M(H)$, taken at 30, 50, and 60 K for $SeMnO_3$. The hysteresis loop measured at 30 K shows the contribution of the spontaneous magnetization that is associated with the ferrimagnetic Mn_3O_4 phase [55], while at 50 and 60 K we observed vanishing of the hysteresis loop and the presence of a paramagnetic state at higher temperature, respectively. From this experimental evidence, we confirm the behaviour of a WFM at about 52 K, as has been proposed by Khon *et al* [31]. Although these data show a WFM, we suggest that the small FM component observed to 52 K could arise from AFM ordering with a canting of the Mn spins due to the strong [M–O_6] octahedral distortion observed in the solid solution.

Figure 7 shows the temperature dependence of the inverse magnetic susceptibility, $1/\chi(T)$, from 300 to 2 K for each x. In this range, the temperature dependence of the inverse magnetic susceptibility is well described by the Curie–Weiss law, $\chi = C/(T - \theta_W)$ where C is the Curie constant and θ_W is the Weiss constant. Table 3 shows the values of μ_{eff} and θ_W that are fitted in the temperature range of 75–300 K. We observed that the effective magnetic moment values, μ_{eff}, are 1.9 μ_B and 7.0 μ_B for $SeCuO_3$ and $SeMnO_3$ respectively; these are in good agreement

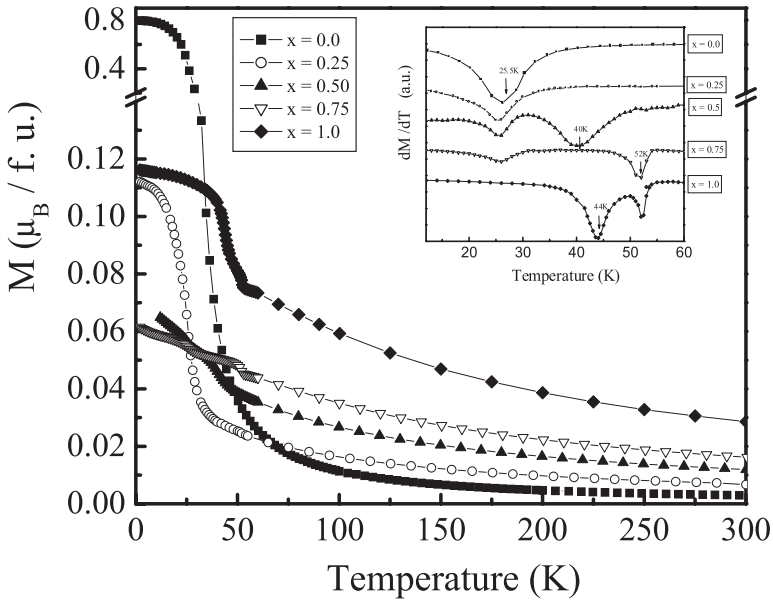

Figure 5. Magnetization as a function of temperature for the $Se(Cu_{1-x}Mn_x)O_3$ samples. The inset shows the derivative of the magnetization, dM/dT, for all compositions.

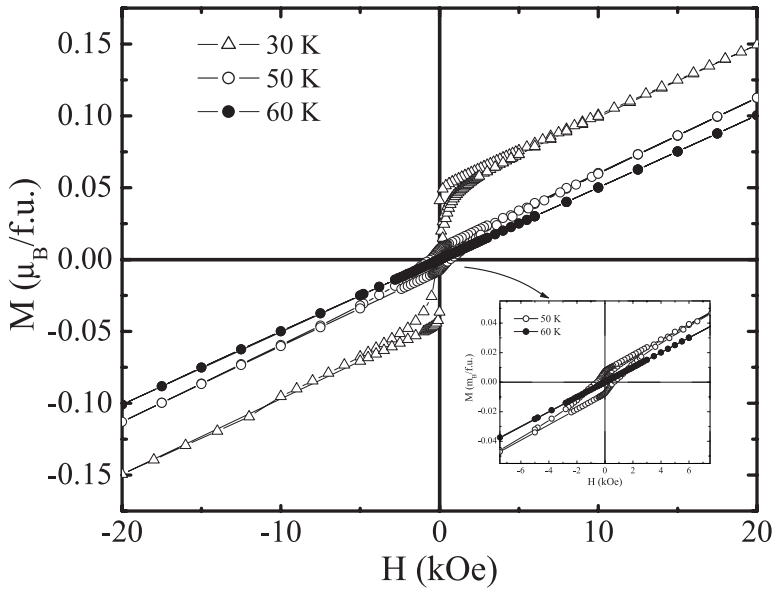

Figure 6. $M(H)$ curves, taken at 30, 50, and 60 K for $SeMnO_3$.

with values from previous studies [31]. The inset of figure 7 shows the Weiss temperature θ_W (derived from the inverse magnetic susceptibility data) as a function of the Mn content. We can observe that the change from a positive to a negative Weiss constant occurs at a very low doping level in $Se(Cu_{1-x}Mn_x)O_3$. Our study does not include doped samples below $x = 0.25$; however, we fitted a potential function of θ_W for each concentration and found that θ_W changes

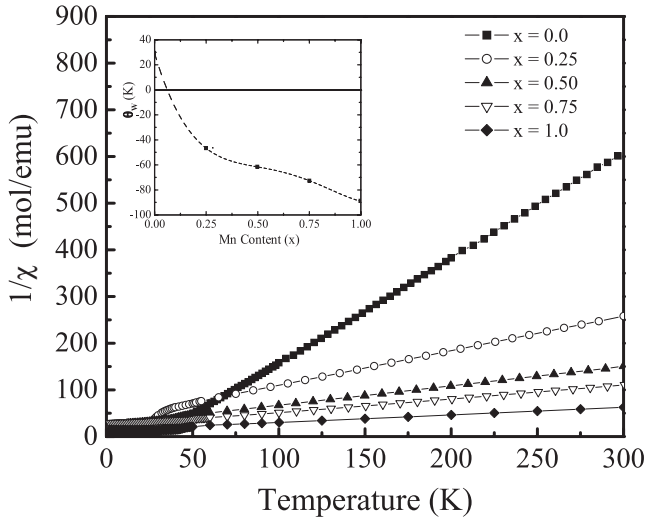

Figure 7. The temperature dependence of the inverse magnetic susceptibility, $1/\chi(T)$.

Table 3. Magnetic parameters of $SeMO_3$ with $M = (Cu_{1-x}Mn_x)$.

x	θ_W (K)	T_N (K)	μ_{eff}
0.0	28.9	—	1.9
0.25	−46.7	—	3.3
0.5	−61.8	40	4.4
0.75	−72.6	51	5.2
1.0	−89.1	44	7.0

from a positive to a negative value when x is close to about 10%. These results suggest a FM-to-antiferromagnetic transition when the doping level exceeds 10% of Mn. However, as we can see in the inset (dM/dT) of figure 5, the FM transition at 25.5 K is present in all doped samples. The more dramatic contrast is for the compound with $x = 0.25$, since only a FM transition signal at 25.5 K is observed in dM/dT even with negative θ_W. This result leads one to question the validity of the Curie–Weiss behaviour and the fundamental proof that there is a ground state coupling between $M = (Cu_{1-x}Mn_x)$ spins, as has been pointed out in other works [51, 57]. The experimental results presented here indicate that the structural parameters are essential to the understanding of the complex interaction in this system.

In order to derive the critical structural parameters which influence the magnetism in the $SeMO_3$ system, two facts must be taken into account: (a) the bond angles remain essentially constant and (b) the octahedral distortion abruptly decreases, both as a function of increasing Mn content. It is likely that the FM–WFM (AFM with canted spins) transition is mainly influenced by the octahedral distortion rather than the tilting, since the M–O(I)–M and M–O(II)–M bond angles change little upon Cu substitution for Mn. Thus, we can assume that the magnetic nature of both bond angles is FM (the presence of the 25.5 K transition) and that the change of sign of θ_W is mainly due to the decrease of the octahedral distortion of [M–O_6] introduced by the substitution of larger Mn (∼1.0 Å) ions in the orthorhombic structure.

Figure 8 shows the dependence on the octahedral distortion (Δ_{oct}) of the Weiss constant (θ_W), derived from the data on structural refinements and the fitting to a Curie–Weiss law. The primary feature in this behaviour is that the Weiss temperature decreases drastically

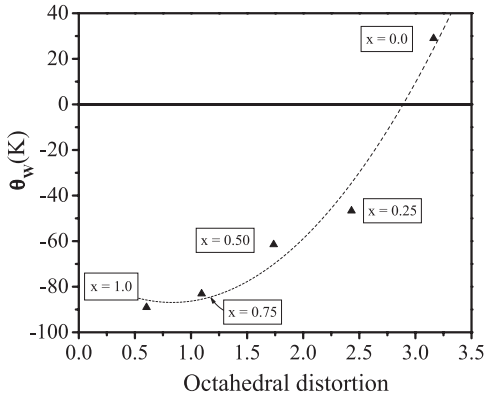

Figure 8. The Weiss constant (θ_W) as a function of Δ_{oct}.

at low doping levels (<25% Mn). For intermediate concentrations the drop of the Weiss temperature is less drastic and it reaches a value of ∼90 K for $SeMnO_3$. This clearly shows that octahedral distortion, in the first instance, can explain the magnetic properties of this solid solution; however, we do not rule out the effect of cation size disorder via changes of the local environments of [M–O_6] octahedra, which can play a significant role in the magnetic properties, as has been suggested in other works [51].

4. Conclusions

In summary, we have presented a detailed crystallographic and magnetic characterization of the $Se(Cu_{1-x}Mn_x)O_3$ system by studying powder XRD patterns at room temperature and magnetization measurements. X-ray diffraction results indicate that the Mn ions occupy the Cu sites of the $Se(Cu_{1-x}Mn_x)O_3$ structure. This replacement causes significant changes in the M–O bond lengths that induce a decrease in the octahedral distortion, which is practically absent in perovskite-type $SeMnO_3$. In contrast, the angles of the bonds remain essentially constant. The magnetic results show that the substitution of Cu for Mn in $SeCuO_3$ has a large effect on the magnetization. Replacing a small amount of Cu by Mn drastically suppresses the saturation moment and changes the sign of the magnetic interaction parameter θ_W. We found a WFM phase in the $SeMnO_3$ compound, probably due to strong octahedral distortion. Additionally, we suggest that it is due to canting spins in the orthorhombic structure that a smaller magnetic component is observed at 52 K.

Acknowledgments

We would like to thank Dr Jose Manuel Gallardo for assistance in sample preparation, Dr Francisco Morales Leal for assistance with the magnetic measurements and Dr Manuel de Llano for helping with the manuscript preparation. This work was supported by CONACYT (Mexico) and CICYT MAT-2001 (Spain).

References

[1] Bednorz J G and Müller K A 1986 *Z. Phys.* B **64** 189
[2] Kusters R M, Singleton J, Keen D A, McGreevy R and Hayes W 1989 *Physica* B **155** 362

[3] Chahara K, Ohno T, Kasai M and Kozono Y 1993 *Appl. Phys. Lett.* **63** 1990
[4] von Helmolt R, Wecker J, Holzapfel B, Schultz L and Samwer K 1993 *Phys. Rev. Lett.* **71** 2331
[5] Jin S, Tiefel T H, McCormack M, Fastnacht R A, Ramesh R and Chen L 1994 *Science* **264** 413
[6] Tokura Y, Urushibara A, Moritomo Y, Arima T, Asamitsu A, Kido G and Furukawa N 1994 *J. Phys. Soc. Japan* **63** 3931
[7] Asamitsu A, Moritomo Y, Tomioka Y, Arima T and Tokura Y 1995 *Nature* **373** 407
[8] Tokura Y, Tomioka Y, Kuwahara H, Asamitsu A, Moritomo Y and Kasai M 1996 *J. Appl. Phys.* **79** 5288
[9] Zener C 1951 *Phys. Rev.* **82** 403
[10] Anderson P W and Hasegawa H 1955 *Phys. Rev.* **100** 675
[11] de Gennes P-G 1960 *Phys. Rev.* **118** 141
[12] Vleck J H V 1939 *J. Chem. Phys.* **7** 72
[13] Kanemori J 1960 *J. Appl. Phys. Suppl.* **31** 14S
[14] Kugel K I and Khomskii D I 1982 *Usp. Fiz. Nauk* **136** 621
[15] Wollan E O and Koehler W C 1955 *Phys. Rev.* **100** 545
[16] Goodenough J B 1955 *Phys. Rev.* **100** 564
[17] Cyrot M and Lyon-Caen C 1975 *J. Physique* **36** 253
[18] Ito Y and Akimitsu J 1976 *J. Phys. Soc. Japan* **40** 1333
[19] Akimitsu J and Ito Y 1976 *J. Phys. Soc. Japan* **40** 1621
[20] Andersson S, Aström K A, Galy J and Meunier G 1973 *J. Solid State Chem.* **6** 187
[21] Galy J, Meunier G, Andersson S and Aström K A 1975 *J. Solid State Chem.* **13** 147
[22] Galy J and Enjalbert R 1982 *J. Solid State Chem.* **44** 1
[23] Meunier G, Svensson C and Carpy A 1976 *Acta Crystallogr.* B **32** 2664
[24] Meunier G, Bertaud M and Galy J 1976 *J. Appl. Crystallogr.* **9** 364
[25] Elenberger H and Pertlik F 1986 *Monatsh. Chem.* **117** 887
[26] Giester G and Wildner M 1991 *J. Solid State Chem.* **91** 370
[27] Wildner M and Langer K 1994 *Phys. Chem. Minerals*
[28] Wildner M 1992 *Acta Crystallogr.* C **48** 595
[29] Wildner M 1993 *J. Solid State Chem.* **103** 341
[30] Wildner M 1994 *J. Solid State Chem.* **113** 252
[31] Kohn K, Inoue K, Horie O and Akimot S 1976 *J. Solid State Chem.* **18** 27
[32] Meunier G, Bertaud M and Galy J 1974 *Acta Crystallogr.* B **30** 2834
[33] Gattow V 1958 *Acta Crystallogr.* **11** 377
[34] Meunier G and Bertaud M 1974 *Acta Crystallogr.* B **30** 2840
[35] Zener C 1951 *Phys. Rev.* **82** 403
[36] García-Muñoz J L, Fontcuberta J, Suaaidi M and Obradors X 1996 *J. Phys.: Condens. Matter* **8** L787
[37] Rodríguez-Martínez L M and Attfield J P 2000 *Phys. Rev.* B **63** 24424
[38] Rodríguez-Martínez L M and Attfield J P 1996 *Phys. Rev.* B **54** R15622
[39] Mazin and Singh D J 1997 *Phys. Rev.* B **56** 2556
[40] Attfield J P, Kharlanov A L and McAllister J A 1998 *Nature* **394** 157
[41] Anderson P W 1950 *Phys. Rev.* **79** 705
[42] Kanemori J 1959 *J. Phys. Chem. Solids* **10** 87
[43] Subramanian M A, Ramirez A P and Marshall W J 1999 *Phys. Rev. Lett.* **82** 1558
[44] Howard C J, Hunter B A and Swinkels D A J 1997 *Rietica IUCR Powder Diffract.* **22** 21
[45] Wills A S and Brown I D 1999 VaList, CEA, France; program available from ftp://ftp.ill.fr/pub/dif/valist/
[46] Shannon R D 1976 *Acta Crystallogr.* A **32** 751
[47] Bauer W H 1981 *Structure and Bonding in Crystals* vol 2 (New York: Academic) pp 31–52
[48] Shannon R D, Gumerman P S and Chenavas J 1975 *Am. Mineral.* **60** 714
[49] Geller S 1956 *J. Chem. Phys.* **24** 1236
[50] Blasco J, Ritter C, García J, de Teresa J M, Pérez-Cacho J and Ibarra M R 2000 *Phys. Rev.* B **62** 9
[51] He T, Huang Q and Cava R J 2000 *Phys. Rev.* B **63** 24402
[52] Okazaki A and Suemune Y 1961 *J. Phys. Soc. Japan* **16** 176
[53] Hanke K, Kupcik V and Lindqvist O 1973 *Acta Crystallogr.* B **29** 963
[54] Escamilla R, Gallardo-Amores J M, Morán E and Alario-Franco M A 2002 *J. Solid State Chem.* **168** 149
[55] Guo L W, Peng D L, Makino H, Inaba K, Ko H J, Sumiyama K and Yao T 2000 *J. Magn. Magn. Mater.* **213** 321
[56] Geller S 1971 *Acta Crystallogr.* B **27** 821
[57] Yoshimura K, Imai T, Kiyama T, Thurber K R, Hunt A W and Kosuge K 1999 *Phys. Rev. Lett.* **83** 4397